Development of the pulse peak from peak-truncated Gaussian optical pulses in a serial array of high-Q ring resonators

Development of the pulse peak from peak-truncated Gaussian optical pulses in a serial array of high-Q ring resonators

Makoto Tomita, Taichi Sudo, Kota Yoshimura, and Daiki Sugio
Department of Physics, Faculty of Science, Shizuoka University, 836, Ohya, Suruga-ku, Shizuoka, 422–8529, Japan

(Received 19 May 2020; accepted 17 September 2020; published 9 October 2020)

We experimentally examined the propagation of a Gaussian-shaped temporal pulse through a serial array of ring resonators, truncating the pulse before its peak. We observed the process whereby a smooth pulse peak related to the Gaussian pulse emerged even when the incident pulse was truncated before its peak, as the pulse passed through an increasing number of ring resonators. The peak emerged when the negative group delay accumulated beyond the pulse truncation time point. This result demonstrated that the earlier portion of the input pulse envelope developed into a smooth Gaussian-shaped pulse peak in the superluminal pulse in good agreement with the analyses based on the instantaneous spectrum. We also discussed the propagation of truncated pulses in a slow light system, where the peak disappeared in the output pulse despite the peak in the input pulse.

DOI: 10.1103/PhysRevA.102.043507

I. INTRODUCTION

Superluminal velocities are ubiquitous effects that appear in a wide variety of photonic systems [1]. Historically, Chu and Wong examined the pulse velocity in GaP:N with a laser tuned to the bound A-exciton line and observed superluminal pulse propagation through the sample with little distortion in the pulse shape [2]. Wang *et al.* demonstrated distortionless superluminal pulse propagation in lossless-linear anomalous dispersion in the double gain lines in Cs gas [3]. The barrier traversal time of optical pulses through a one-dimensional photonic band-gap material has been found to become superluminal and independent of barrier thickness [4]. Superluminal velocities are observed in high-Q resonators [5] and quantum manipulated materials with steep refractive index profiles [6,7]. The peaks of the superluminal pulses appear at a time exactly predicted by the conventional definition of group velocity,v_g, indicating that the conventional definition still holds in these conditions [8]. Superluminal pulse propagation seemingly contradicts the causality of Einstein's theory of special relativity; however, it is understood that the arrival of the smooth pulse peak can be predicted on the basis of the expansion of the early part of the pulse, such that the arrival of the smooth superluminal pulse peak does not contain true information [9–11].

Among superluminal velocity phenomena, negative velocity is a highly unusual effect. A negative velocity indicates that the peak of the input pulse emerges from the opposite side of the sample at an instant before the peak of the pulse enters the sample. Because this observation seemingly contradicts more general causality (i.e., the cause occurs before the result), this naturally leads to the question of whether it is possible to observe the pulse peak at the output even when the pulse is truncated to remove its later part, such that the input pulse lacks the peak. Recently, using a single-stage resonator, a Gaussian-shaped peak was shown to emerge from the far side of a negative group-velocity medium, although the incident pulse was terminated before its peak [12]. Although this experiment confirmed that the appearance of the smooth Gaussian-shaped pulse peak in the negative group velocity medium is a gradual analytic continuation of the earlier portion of the input pulse envelope, it was unclear how the pulse peak developed during propagation.

Our motivation here was to investigate the development of pulse peaks from peak-truncated Gaussian-shaped temporal pulses in the context of the above question. Specifically, we employed a ring resonator that provided a dynamic recurrent system [13,14]. This system was used in previous investigations of pulse propagation over long distances. It was shown that the saddle-point method [8], as well as the concepts of net and reshaping delay [15,16], are applicable to pulse propagation even when the pulses propagate through a large number of resonator stages. However, our interest in this paper is in the pulse peak. Using this system, we measured the transmitted pulse profiles as a function of the recurrence time N, where N is the number of times that a pulse passed through the resonator. We observed the process whereby a smooth pulse peak related to the Gaussian pulse emerged, as the pulse passed through an increasing number of ring resonators. The peak emerged when the negative group delay accumulated beyond the pulse truncation time point. We also examined propagation of truncated Gaussian pulses in a slow light system. In the slow light system, the smooth Gaussian peak disappeared at the truncation time point, even when input pulses had a Gaussian peak.

The peak-truncated pulse used in our experiment could achieve an instantaneous spectrum, which is defined mathematically as the momentary spectrum that the dispersive medium "perceives" at each instant while the medium is interacting with the pulse [17]. The instantaneous spectrum has different spectral content from the original input pulse, and the content depends on the time instant considered. Peatross

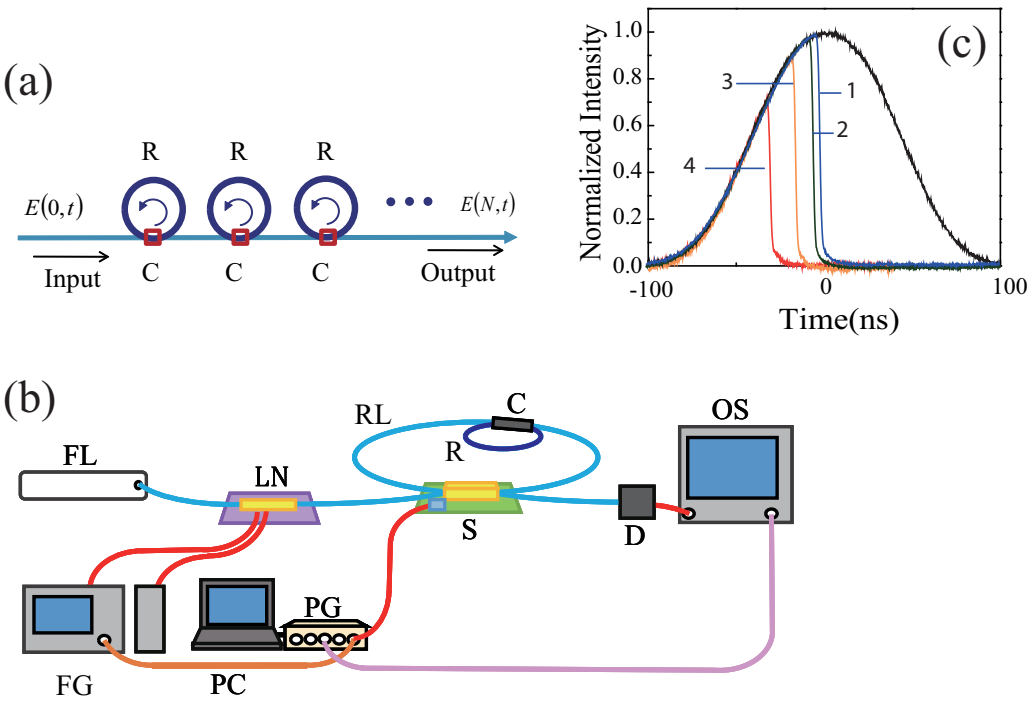

FIG. 1. (a) Conceptual illustration of a serial array of ring resonators. *R* is a ring resonator; *C* is a coupler. (b) Schematic diagram of experimental setup. *FL*, fiber laser; *LN*, $LiNbO_3$ modulator; *S*, 2 × 2 fast optical switch; *C*, coupler; *R*, ring resonator; *RL*, fiber recurrent loop; *D*, detector; *FG*, function generator; *PC*, computer; *OS*, oscilloscope. (c) Colored lines are peak-truncated Gaussian pulse profiles used in experiments. Truncation time is indicated by line 1, $t_{NA} = -4$ ns; line 2, −8 ns; line 3, −19 ns; and line 4, −32 ns, respectively. Black line represents original Gaussian pulse.

et al. discussed superluminal and ultraslow pulse propagation on the basis of the instantaneous spectrum [17]. The present experimental results are in good accordance with that of the analyses based on the instantaneous spectrum, i.e., a linear system responds to the pulse up to the present time as though at any moment the pulse will suddenly cease.

II. EXPERIMENTS

The concept of a serial array of ring resonators is illustrated schematically in Fig. 1(a). A single-stage resonator is insufficient to emulate pulse propagation through resonator systems, because single-stage resonators interact with electromagnetic waves only once. Coupled resonator optical waveguides [18] or side-coupled integrated sequences of spaced optical resonators [19] may be suitable systems to examine the propagation effect. However, it is extremely difficult to prepare resonators with exactly the same resonance frequency and Q value. Here, we employed an alternative approach based on a recently developed method that uses a dynamic recurrent system [13,14].

The experimental setup was similar to that used in Ref. [14] and is illustrated in Fig. 1(b). Briefly, a 1550-nm Er-fiber laser was used as the incident light source; the fine-laser frequency was controlled through the cavity length in the fiber laser. The spectral width was 1 kHz. A $LiNbO_3$ modulator was used; both a smooth Gaussian-shaped temporal pulse and truncated Gaussian-shaped pulses were prepared. The pulse was truncated at four time positions before its peak. The slowly varying envelope of the truncated input was Gaussian until the time at which it was truncated, t_{NA}; then, it dropped to zero to remove the back of the pulse:

$$\tilde{E}_{\rm in}(t) = \Theta(t)\exp\left[-\left(\frac{t}{t_p}\right)^2\right], \quad \Theta(t) = \begin{cases} 1 & t < t_{NA} \\ 0 & t \geqslant t_{NA} \end{cases}. \quad (1)$$

Note that the function is discontinuous at the truncation time point; hence, this point behaves as a nonanalytical point. In our experiments, this nonanalytical point was a special time point where, in the fast light system, the hidden part of the pulse profiles emerged as a result of the analytic connection of the early part of the pulse envelope. In the slow light system, this point also acted as a special time point where parts of the input pulse corresponding to the group delay time became hidden. The pulse duration was $t_p = 91$ ns. Curves 1, 2, 3, and 4 in Fig. 1(c) show truncated input pulses used in the experiments, with truncation times $t_{NA} = -4$, −8, −19, and −32 ns, respectively. For the dispersive media, fiber ring resonators were used. The dispersion of a ring resonator is highly controllable via the cavity loss parameter, x, and coupling parameter, y [20]. The output light electric field, $\tilde{E}_{\rm out}(t)$, normalized by the incident light electric field, is given as

$$\frac{\tilde{E}_{\rm out}(\omega)}{\tilde{E}_{\rm in}(\omega)} = (1-\gamma)^{1/2}\left[\frac{y - x\exp(i\varphi)}{1 - xy\exp(i\varphi)}\right] = \sqrt{T(\omega)}\exp\left(i\theta(\omega)\right), \quad (2)$$

where γ is the excess loss at the coupler and $\varphi(\omega)$ is the one-round phase shift in the ring resonator. The transmission intensity $T(\omega)$ shows a periodic dip structure as a function of incident laser frequency. For the undercoupling condition

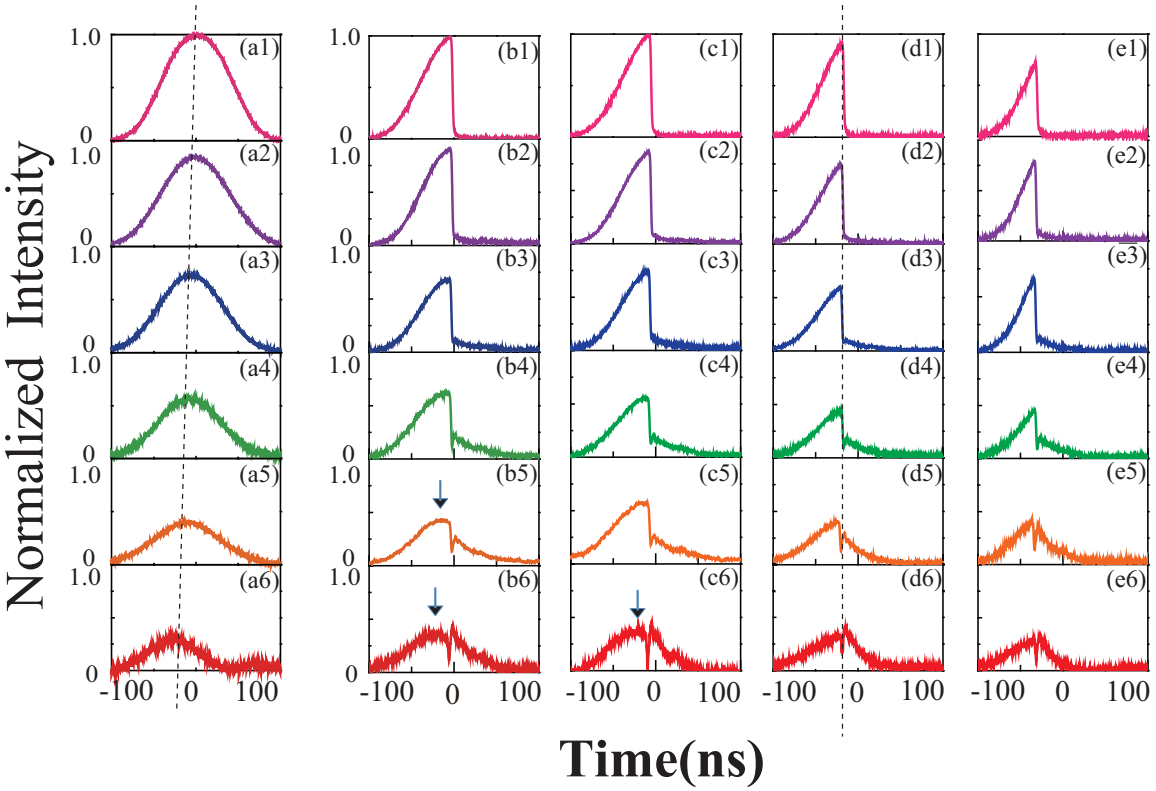

FIG. 2. (a) Observed transmitted pulse profiles for the smooth Gaussian-shaped input pulse for different N in undercoupled ring resonator (i.e., fast light system). Numbers of times that a pulse passed through the resonator were as follows: (a1) $N = 0$ (input pulse), (a2) 1, (a3) 2, (a4) 3, (a5) 4, and (a6) 5. (b)–(e) depict transmitted pulse profiles for peak-truncated input pulses for different N (from top to bottom, $N = 0$ to 5 in all columns). Truncation times were (b) $t_{NA} = -4$ ns, (c) -8 ns, (d) -19 ns, and (e) -32 ns, respectively. All intensities were normalized with respect to maximum of smooth Gaussian pulse. Black downward arrows in (b5), (b6), and (c6) indicate emerged peaks. Dashed black inclined line in (a) shows position of pulse peak as a guide. Dashed black vertical line in (d) represents position of truncation times.

($x < y$), the transmitted phase shift $\theta(\omega)$ shows anomalous dispersion at the center of the resonances. The group delay is negative $\tau_g = \partial\theta/\partial\omega < 0$, which corresponds to superluminal pulse propagation. For the overcoupling condition ($x > y$), $\theta(\omega)$ shows normal dispersion. In the present experiment, a 98:2 coupler ($y^2 = 0.98$) was used to achieve undercoupling conditions. The physical length of the ring was $L_R = 1.0$ m, and the resonance width was $\Delta\nu_R = 6.7$ MHz.

The dynamic recurrent system was constructed using fast optical switch that provided two input ports and two output ports (2 × 2 optical switch). The recurrent loop consisted of $L_{RL} = 500$ m optical fiber; hence, the recurrent time (i.e., round-trip time for the pulse in the recurrent loop) was $\tau = L_{RL}/c$, ~2500 ns. The response times of the optical switches were 70 ns. When the input optical pulse arrived at the optical switch, the switch opened and injected the optical pulse into the recurrent loop. Then, the switch closed and the pulse was confined in the recurrent loop. At time $T_N = N\tau$, where N is the circulation time in the loop, the switch reopened. The pulse was then extracted from the recurrent loop after N circulation times and the pulse shape was examined using an InGaAs photodetector and a digital oscilloscope.

Column (a) in Fig. 2 shows the transmitted pulse profile observed with the smooth Gaussian input pulse after passing through the ring resonator N times under on-resonance conditions. Figure 2(a1) shows the pulse profile for $N = 0$ (i.e., input pulse). Figure 2(a2) shows the profile for $N = 1$. As the undercoupled ring resonator exhibited anomalous dispersion, the pulse peak was advanced by -2.5 ns. As the number N increased, the pulse peak advanced by a constant rate of -3.1 ns/stage. Open circles in Fig. 3 summarize the peak advancement as a function of N for the smooth Gaussian pulse. Column (b) in Fig. 2 shows the transmitted pulse profile observed with the peak-truncated input pulse, following passage through the ring resonator N times. The truncation time was $t_{NA} = -4$ ns [line 1 in Fig. 1(c)]. As N increased, the overall pulse profile shifted toward the negative time region [Figs. 2(b2) and 2(b3)]. When $N < 2$, the Gaussian peak was not observed; however, for $N = 4$ and 5, the wing of the smooth Gaussian pulse tail from the pulse peak grew, such that the Gaussian pulse peak eventually emerged [black downward arrows in Figs. 2(b5) and 2(b6)]. Output peaks observed with the peak-truncated input pulses at $N = 4$ and 5 were located at -12.7 and -16.2 ns, respectively. These times were the same advancement as that observed for the smooth Gaussian pulse. Column (c) in Fig. 2 shows the transmitted pulse profile observed with the input pulse truncated at $t_{NA} = -8$ ns [line 2 in Fig. 1(c)]. In this instance, the Gaussian peak was not observed for $N < 3$. However, a Gaussian pulse peak was observed at $N = 5$ [black downward arrows in Fig. 2(c6)]. Columns (d) and (e) in Fig. 2 show the transmitted pulse profile observed with pulses truncated at $t_{NA} = -19$ and -32 ns

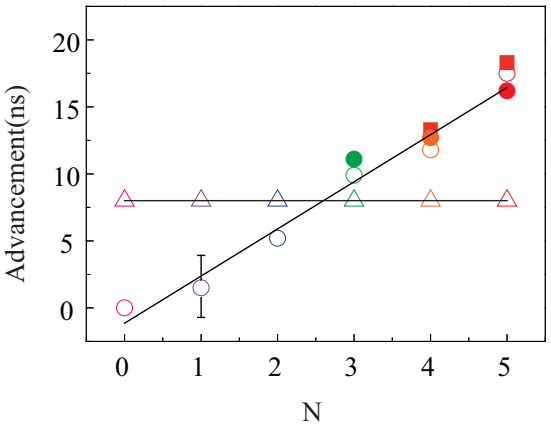

FIG. 3. Open circles represent advancement of pulse peak for the smooth Gaussian pulse as a function of N in undercoupled ring resonator. Solid circles at $N = 3$, 4, and 5 are peak positions observed with peak-truncated pulses. Truncation time was $t_{NA} = -4$ ns [corresponding to Figs. 2(b4), 2(b5), and 2(b6), respectively]. Solid squares at $N = 4$ and 5 are peak positions observed with peak-truncated pulses. Truncation time was $t_{NA} = -8$ ns [corresponding to Figs. 2(c5) and 2(c6)]. Open triangles represent position of pulse truncation point in output pulses as a function of N observed with peak-truncated pulse, at truncation time of $t_{NA} = -8$ ns [corresponding to Fig. 2(d)].

[lines 3 and 4 in Fig. 1(c)], respectively. In these instances, although similar behavior was observed in that the overall pulse profile shifted toward the negative time region, the output pulse peak was not observed within $N < 5$. Dashed black vertical lines in column (d) in Fig. 2 show the positions of the truncation times; pulse truncation points were neither advanced nor delayed. This point acts as a nonanalytical point where the hidden part of the pulse profiles emerged.

To confirm the experimental results, we performed a numerical simulation using the same parameters as those applied in the experiments. Loss and coupling parameters were $x = 0.85$ and $y = 0.99$ ($y^2 = 0.98$). Column (a) in Fig. 4 shows the transmitted pulse profile calculated with the smooth Gaussian input pulse, following passage through the ring resonator N times. As the number N increased, the advancement of the pulse peak increased linearly. Column (b) in Fig. 4 shows the transmitted pulse profile calculated with the peak-truncated Gaussian input pulse, where the truncation time was $t_{NA} = -4$ ns after passing N times. With increasing N, the peak emerged for $N = 4$ and 5 [Fig. 4(b5) and 4(b6)]. This calculation confirms that under the condition $\tau_g < t_{NA} \leqslant 0$, where τ_g is the pulse advancement, a smooth Gaussian peak appears in the output pulse, even when the input pulse does not exhibit a Gaussian peak. This is in excellent agreement with the experimental results shown in Fig. 2.

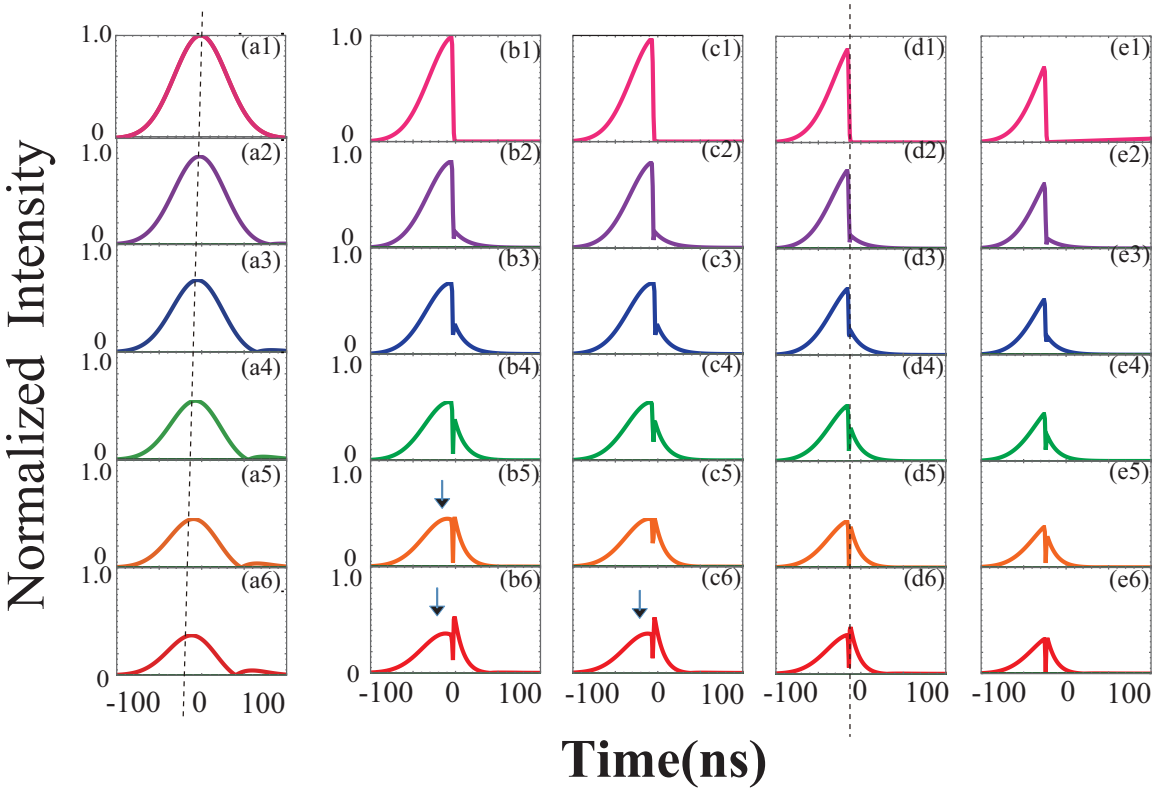

FIG. 4. Calculated temporal pulse profiles of transmitted pulses for different N in undercoupled ring resonator (i.e., fast light system). Input pulses were (a) smooth Gaussian-shaped pulses and (b)–(e) peak-truncated pulses, corresponding to graphs in Fig. 2. All intensities were normalized with respect to maximum of smooth Gaussian pulse. Dashed black inclined line in (a) shows position of pulse peak as a guide. Dashed black vertical lines in (d) represent position of truncation time. Time origin $t = 0$ was set at pulse peak time.

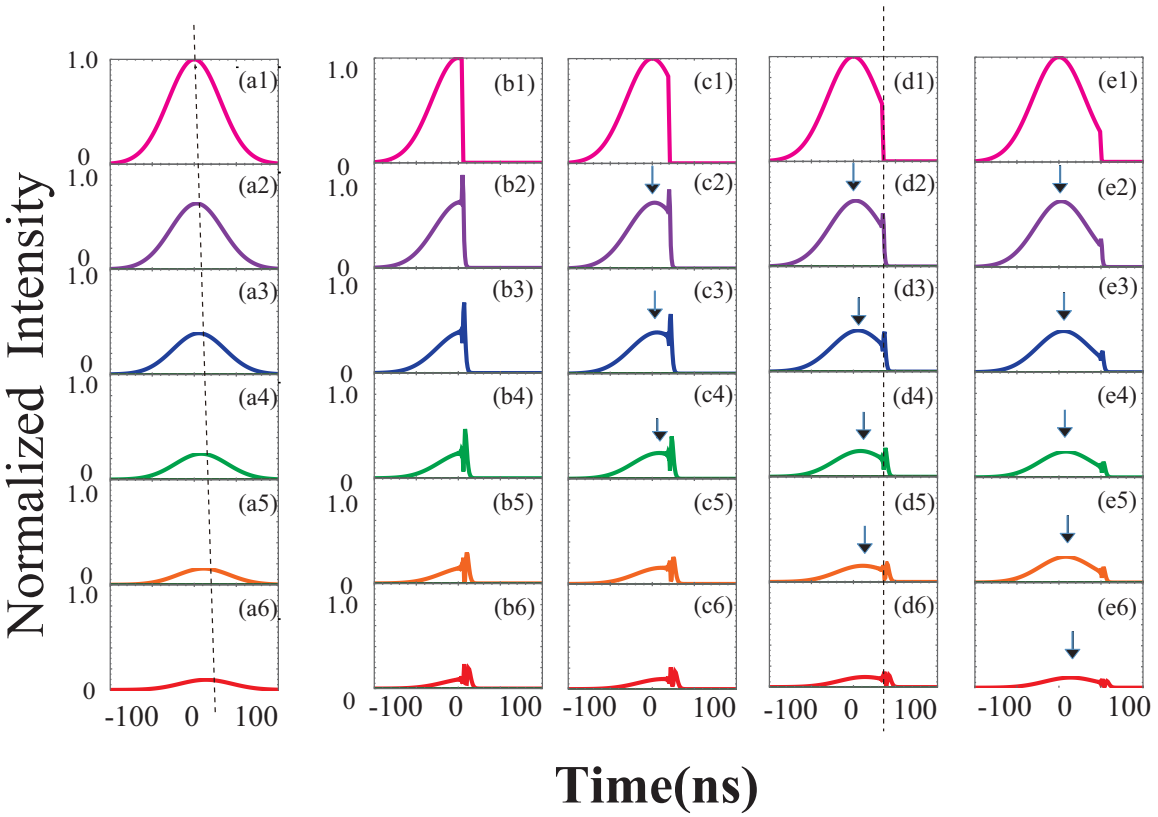

FIG. 5. (a) Calculated transmitted pulse profiles for the smooth Gaussian-shaped input pulse for different numbers of resonators N in overcoupled ring resonator (i.e., slow light system). Numbers of times that a pulse passed through the resonator were as follows: (a1) $N = 0$ (input pulse), (a2) 1, (a3) 2, (a4) 3, (a5) 4, and (a6) 5. (b)–(e) depict calculated transmitted pulse profiles for truncated input pulses for different N (from top to bottom, $N = 0$ to 5 in all columns). Truncation times were (b) $t_{NA} = +5$ ns, (c) +20 ns, (d) +35 ns, and (e) +50 ns, respectively. Black downward arrows indicate peaks. Dashed black vertical lines in (d) represent positions of truncation times.

III. DISCUSSION

In the previous sections, we examined the pulse peak in a fast light system. It is also of interest to examine the peak in a slow light system; hence, we simulated the propagation of truncated pulses under these conditions. Column (a) in Fig. 5 shows the transmitted pulse profile for the smooth Gaussian input pulse, following passage through different numbers of resonators N. The loss and coupling parameters were $x = 0.95$ and $y = 0.8$. Hence, the ring resonators were prepared in the overcoupling condition (i.e., a slow light system). As the number N increased, the delay in pulse peak increased linearly. Column (c) in Fig. 5 shows the calculated transmitted pulse profile for the input pulse truncated at $t_{NA} = +20$ ns. With increasing N, the Gaussian pulse peak shifted toward the later time region; the peak disappeared when it reached truncation time t_{NA} [$N = 4$ and 5; Figs. 5(c5) and 5(c6)]. Columns (d) and (e) in Fig. 5 show similar results for the transmitted pulse profile calculated for input pulses truncated at $t_{NA} = 35$ and 50 ns, respectively. In these calculations, the smooth Gaussian peak in the truncated pulse survived in the output pulse, even for $N = 4$ and 5.

As the situation shown in Fig. 5 is the opposite to the case of peak creation from a peak-truncated input pulse, we briefly demonstrated the annihilation of the pulse peak at the output side in a slow light system. Figure 6(a) shows the experimental results of the transmitted pulse profile observed with the truncated Gaussian input pulse in an overcoupled ring

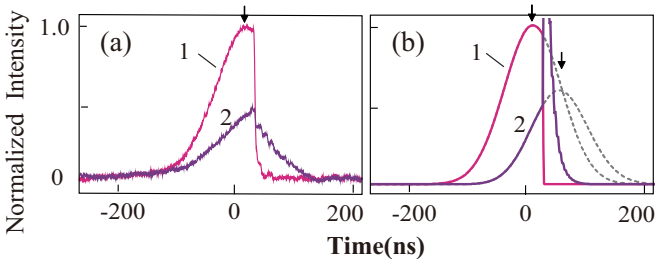

FIG. 6. (a) Observed transmitted pulse profiles for truncated input pulses in an overcoupled ring resonator (i.e., slow light system; $N = 1$). Curves 1 and 2 are the input and transmitted pulses, respectively. The truncation time was $t_{NA} = 15$ ns. (b) Calculated temporal pulse profiles of transmitted pulses. Curves 1 and 2 are the input and transmitted pulses, respectively. The dotted lines indicate the input and transmitted temporal profiles, respectively, when the smooth Gaussian-shaped pulse was not truncated. All intensities were normalized with respect to the maximum of the input pulse. Black downward arrows indicate peaks.

resonator with an 80:20 coupler ($y^2 = 0.8$). Curve 1 is the input pulse. The pulse duration of the original Gaussian pulse was $t_p = 120$ ns and the pulse was truncated after $t_{NA} = 15$ ns. As this occurs after the pulse peak, the input pulse has a peak related to the Gaussian pulse. As the overcoupled ring resonator exhibited normal dispersion, the pulse peak was expected to be delayed by $\tau_g = 40$ ns. Curve 2 in Fig. 6(a) shows the transmitted pulse profile. The experimental results showed that the peak disappeared at the output side of the medium, even when the incident pulse had a peak. Figure 6(b) shows the calculated temporal pulse profiles. Curves 1 and 2 are the input and transmitted pulses, respectively. The calculation showed good agreement with the experimental result, in that the peak disappeared at the output side of the medium. The large transient spike after truncation in the simulation [Fig. 6(b)] was not seen in the experiments [Fig. 6(a)], which may be attributed to the finite time resolution of the experiments.

To summarize the experiments and simulations, we categorized the results into four cases, depending on dispersion and pulse truncation time. Case I is a fast light system with the input pulse truncated before the pulse peak (i.e., $t_{NA} < 0$). In this case, two situations are possible. First, when the dispersion is strong or the propagation distance (i.e., N) is sufficiently long—pulse advancement τ_g is large as $\tau_g < t_{NA} < 0$—a Gaussian-shaped peak emerges at the truncation time point in the output pulse, even when the incident pulse was truncated before its peak. This is the situation shown in columns (b) and (c) in Fig. 2. In contrast, when the dispersion is weak or propagation distance is short, such that the pulse advancement is small compared to the truncation time as $t_{NA} < \tau_g < 0$, the peak does not appear from the output side. This is the situation illustrated in columns (d) and (e) in Fig. 2. Case II represents a fast light system, in which the input pulse is truncated after the pulse peak (i.e., $0 < t_{NA}$). In this case, the input pulse has a peak, which is simply advanced by τ_g in the output pulse. This is a trivial case. In case III, the system is a slow light system, in which the input pulse is truncated before the pulse peak (i.e., $t_{NA} < 0$). In this case, the input pulse and output pulses both have no peak. Finally, case IV is a slow light system with an input pulse that is truncated after the pulse peak. (i.e., $0 < t_{NA}$). In this case, the input pulse has a peak. When the dispersion is weak or the propagation distance is short, such that the pulse delay is small as $0 < \tau_g < t_{NA}$, the peak remains in the output pulse. This is the situation illustrated in columns (d) and (e) in Fig. 5. In contrast, when the dispersion is strong and the pulse delay τ_g is large as $0 < t_{NA} < \tau_g$, the peak disappears at the output side of the medium, even when the incident pulse has a peak. This is the situation illustrated in Figs. 5(b) and 5(c).

IV. SUMMARY

In summary, we experimentally investigated the development of pulse peaks from peak-truncated Gaussian-shaped temporal pulses during propagation in a fast light system, by using a ring resonator that provided a dynamic recurrent system. We observed that a smooth pulse peak related to the Gaussian pulse arose at the pulse truncation time point as the number of ring resonators that the pulse passed through increased, despite the absence of an input pulse peak. We also performed simulations to examine the propagation of the truncated Gaussian-shaped temporal pulses in a slow light system. Under the condition where $0 < t_{NA} < \tau_g$, the smooth Gaussian peak disappeared at the pulse truncation time point, although the input pulse had a Gaussian peak.

The creation of a Gaussian pulse peak from a peak-truncated pulse may also be possible in other physical systems, including coupled resonator optical waveguides [17], side-coupled integrated sequences of spaced optical resonators [18], and even coherently controlled atomic systems [6,7]. These structures have applications in fundamental physics and telecommunication systems [1]. Although the basic mechanism to generate the pulse peak may be similar, there may also be some differences. For example, the effects of the backward-traveling waves may be significant depending on the physical system [21,22]. Regeneration of the pulse peak from the peak-truncated pulse may have application to *Planaria* photons that exhibit an extremely well-developed ability to regenerate lost pulse parts during propagation.

ACKNOWLEDGMENTS

This work was supported by Japan Society for the Promotion of Science (JSPS) KAKENHI Grant No. JP18H01150.

[1] P. W. Milonni, *Fast Light, Slow Light and Left-Handed Light* (Taylor & Francis, New York, 2004).

[2] S. Chu and S. Wong, Linear Pulse Propagation in an Absorbing Medium, Phys. Rev. Lett. **48**, 738 (1982).

[3] L. J. Wang, A. Kuzmich, and A. Dogariu, Gain-assisted superluminal light propagation, Nature (London) **406**, 277 (2000).

[4] V. Laude and P. Tournois, Superluminal asymptotic tunneling times through one-dimensional photonic bandgaps in quarter-wave-stack dielectric mirrors, J. Opt. Soc. Am. B **16**, 194 (1999).

[5] K. Totsuka, N. Kobayashi, and M. Tomita, Slow Light in Coupled-Resonator-Induced Transparency, Phys. Rev. Lett. **98**, 213904 (2007).

[6] M. S. Bigelow, N. N. Lepeshkin, and R. W. Boyd, Superluminal and slow light propagation in a room-temperature solid, Science **301**, 200 (2003).

[7] A. Godone, F. Levi, and S. Micalizio, Slow light and superluminality in the coherent population trapping maser, Phys. Rev. A **66**, 043804 (2020).

[8] A. I. Talukder, Y. Amagishi, and M. Tomita, Superluminal to Subluminal Transition in the Pulse Propagation in a Resonantly Absorbing Medium, Phys. Rev. Lett. **86**, 3546 (2001).

[9] M. D. Stenner, D. J. Gauthier, and M. A. Neifeld, The speed of information in a 'fast-light' optical medium, Nature (London) **425**, 695 (2003).

[10] Y. Morita and M. Tomita, Propagation of phase non-analytical points in fast and slow light media, Phys. Rev. A **96**, 023813 (2017).

[11] G. Diener, Superluminal group velocities and information transfer, Phys. Lett. A **223**, 327 (1996).

[12] M. Tomita, H. Amano, S. Masegi, and A. I. Talukder, Direct Observation of a Pulse Peak Using a Peak-Removed Gaussian Optical Pulse in a Superluminal Medium, Phys. Rev. Lett. **112**, 093903 (2014).

[13] Y. Suzuki and M. Tomita, Development of weak coherent 0π optical pulses in a ring resonator with a dynamic recurrent loop, J. Opt. Soc. Am. B **34**, 489 (2017).

[14] Y. Morita and M. Tomita, Development of superluminal pulse propagation in a serial array of high-Q ring resonators, Sci. Rep. **9**, 14280 (2019).

[15] J. Peatross, S. A. Glasgow, and M. Ware, Average Energy Flow of Optical Pulses in Dispersive Media, Phys. Rev. Lett. **84**, 2370 (2000).

[16] A. I. Talukder, T. Haruta, and M. Tomita, Measurements of Net Group and Reshaping Delays for Optical Pulse in Dispersive Media, Phys. Rev. Lett. **94**, 223901 (2005).

[17] J. Peatross, M. Ware, and S. A. Glasgow, Role of the instantaneous spectrum on pulse propagation in causal linear dielectrics, J. Opt. Soc. Am. A **18**, 1719 (2001).

[18] F. Morichetti, C. Ferrari, A. Canciamilla, and A. Melloni, The first decade of coupled resonator optical waveguides: Bringing slow light to applications, Laser Photonics Rev. **6**, 74 (2012).

[19] J. E Heebner, R. W. Boyd, and Q.-H. Park, SCISSOR solitons and other novel propagation effects in microresonator-modified waveguides, J. Opt. Soc. Am. B. **19**, 722 (2002).

[20] K. Totsuka and M. Tomita, Slow and fast light in a microsphere-optical fiber system, J. Opt. Soc. Am. B **23**, 2194 (2006).

[21] G. M. Gehring, A. Schweinsberg, C. Barsi, N. Kostinski, and R. W. Boyd, Observation of backward pulse propagation through a medium with a negative group velocity, Science **312**, 895 (2006).

[22] A Dogariu, A. Kuzmich, H. Cao, and L. J. Wang, Superluminal light pulse propagation via rephasing in a transparent anomalously dispersive medium, Opt. Express **8**, 344 (2001).